

Theoretical and experimental picosecond photoluminescence studies of the quantum-confined Stark effect in a strongly coupled double-quantum-well structure

C. C. Phillips and R. Eccleston

Solid State Group, Department of Physics, Imperial College of Science and Technology, University of London, London SW7 2AZ, United Kingdom

S. R. Andrews

GEC Research Limited, Hirst Research Centre, East Lane, Wembley, Middlesex HA9 7PP, United Kingdom

(Received 10 May 1989)

Time-resolved photoluminescence measurements as a function of perpendicular applied electric field and temperature are reported in a GaAs-Al_xGa_{1-x}As strongly coupled double-quantum-well (CQW) structure. The excitonic radiative lifetime is found to increase with field at a rate ≈ 3 times faster than previously observed in single-QW structures of the same overall width, and a three-dimensional envelope-function calculation is shown to provide an excellent quantitative description of this effect, demonstrating the validity of this type of calculation for both the energies and oscillator strengths of radiative transitions. Variable temperature experiments are used to probe exciton center-of-mass motion allowing the mean exciton localization area (due to interface fluctuations) to be measured.

I. INTRODUCTION

The linear optical properties of quantum-well structures have been the subject of many studies over recent years. The principal features which have emerged are (a) the modification of the joint optical density of states for interband transitions by the two-dimensional (2D) confinement,¹ (b) the enhancement of the oscillator strength for excitonic transitions due to the increased binding energy of the confined exciton, and (c) the quantum-confined Stark effect (QCSE),² which describes the persistence of exciton transitions at substantially increased applied electric fields compared to the bulk, the ionization of the exciton in the electric field being prevented by the presence of the heterojunction confinement potentials.

Here we report the results of time-resolved photoluminescence (TRPL) studies of the QCSE in a strongly coupled double-quantum-well (CQW) structure. Such structures are formed from two single quantum wells separated by a narrow barrier, typically 1–2 nm in width, and in recent studies^{3–5} they have been shown to behave in a way that is quantum mechanically analogous to the well-known hydrogen-molecule problem. For a sufficiently thin barrier, the degenerate electron and hole eigenstates of the isolated wells hybridize to form symmetric and antisymmetric pair states at lower and higher energy than the degenerate parent states.

The application of a perpendicular electric field increases the coupling between the wells as the effect of the dividing barrier becomes reduced, increasing the energy splitting between the symmetric and antisymmetric states. This symmetry splitting acts to enhance the usual $n=1$ excitonic QCSE shift observed in single-quantum-well structures of similar overall widths, an effect which

makes CQW structures attractive candidates for electro-optic modulator device applications.⁵ Recently reported steady-state luminescence excitation studies⁴ have demonstrated that the behavior of the coupled quantum-well state energies can be quantitatively well described within the theoretical framework of the effective-mass approximation.

The application of a perpendicular field also acts to decrease the effective oscillator strengths of those transitions which are symmetry allowed in zero field, through an increase in both the spatial separation of the electron and hole wave functions in the z direction,⁵ and also the spatial extent of the excitonic wave function in the plane of the wells.⁴

This change in CQW oscillator strength is also enhanced over that in a single QW (Ref. 5) by symmetry splitting, which is consistent with larger Stark shifts. Here we report on the use of time-resolved photoluminescence (TRPL) measurements for the first time to quantitatively study the changing form of both the in-plane and perpendicular components of the excitonic wave function in a CQW structure as a function of applied field. The changes in the in-plane excitonic component alter the calculated oscillator strength of the transition by a factor of ≈ 1.6 over the fields studied here (compared with only a $\approx 9\%$ change in the Stark shifts), and TRPL thus provides a sensitive means of probing 2D-exciton diameters and testing excitonic binding-energy theories. The effect of the center-of-mass motion of the exciton on the absolute radiative lifetimes is also studied, allowing a measurement of the mean island size for monolayer fluctuations at the CQW heterointerfaces.

Previous TRPL measurements on single quantum wells (SQW's) have failed to show the predicted behavior as a function of electric field. In early studies,⁶ a pronounced

decrease in the luminescence lifetime with field was observed and attributed to an increase in nonradiative recombination rates. More recently,^{7,8} the predicted increase in the radiative lifetime has been observed but the magnitude of the increase was significantly smaller than predicted. The enhancement of the QCSE in our CQW's means that in the field regimes of interest, carrier tunneling rates out of the wells are always small compared with radiative exciton decay rates [as evinced by the temperature and field independence of the time-integrated excitonic photoluminescence (PL) efficiency], and radiative lifetimes (and therefore oscillator strengths) are directly measurable with high accuracy.

II. THEORY

A. The form of the excitonic wave function for relative e - h motion

Within the framework of the effective-mass approximation, the exciton envelope wave function is factorized into the form

$$\Phi_{\text{ex}}(x, y, z) = [\varphi_e(z)\varphi_h(z)\exp(-\rho/a)][a(2/\pi)^{1/2}], \quad (1a)$$

where $\varphi_e(z)$ and $\varphi_h(z)$ are the orthonormalized components of the ground-state free-carrier envelope functions in the confinement direction (z). The $\exp(-\rho/a)$ term is a $1s$ -like excitonic envelope function describing the electron-hole correlation, where a is a variational parameter describing the spatial extent of the exciton. Here we have used two expressions for ρ , corresponding to the separable case where the z dependence of the exciton correlation is determined only by the free-carrier envelope terms (the 2D exciton approximation) and ρ is a function of x and y only, and the nonseparable case where a z dependence is included in ρ , i.e.,

$$\begin{aligned} \rho(x, y) &= (x_{eh}^2 + y_{eh}^2)^{1/2}, \quad \text{separable,} \\ \rho(x, y, z) &= (x_{eh}^2 + y_{eh}^2 + z_{eh}^2)^{1/2}, \quad \text{nonseparable,} \end{aligned} \quad (1b)$$

where x_{eh}, y_{eh}, z_{eh} are the relative separations of the electron and hole in the x, y, z directions.

We calculate the free-carrier terms using the tunneling resonance method¹ to find a numerical solution of the one-dimensional (1D) Schrödinger equation to obtain the envelope functions. The perpendicular effective masses used were those of Miller and Kleinmann.⁹ The parameter a is calculated variationally by minimizing $\langle \Phi_{\text{ex}} | H | \Phi_{\text{ex}} \rangle$, where

$$H = \frac{-\hbar^2}{2\mu} \left[\frac{\delta^2}{\delta r^2} + \frac{1}{r} \frac{\delta}{\delta r} \right] + \frac{e^2}{4\pi\epsilon_0\epsilon_r R} \quad (2)$$

with $r = (x_{eh}^2 + y_{eh}^2)^{1/2}$ and $R = (r^2 + z_{eh}^2)^{1/2}$.

We use $\epsilon_r = 12.15$, which is the geometrical average of the background dielectric constants in GaAs and AlGaAs, $x = 0.3$, and $\mu = 0.046m_0$ for the heavy-hole exciton reduced mass using the Luttinger parameters $\gamma_1 = 5.47$, $\gamma_2 = 1.26$, and $\gamma_3 = 0$. This value for μ is intermediate between that measured in magnetorefectivity measurements in single quantum wells of widths 7.7 nm

($\mu = 0.049$) and 11.2 nm ($\mu = 0.045$).¹⁰ We neglect here the effects of light- and heavy-hole mixing¹¹ and the discontinuity of parallel effective masses at the heterojunctions.¹² The exciton radiative lifetime is inversely proportional to the square of the electron-hole overlap integral and in the separable case is given by

$$\tau^{-1} \propto \langle |\Phi_{\text{ex}}(\rho=0)|^2 \rangle_{\text{av}} \propto \langle |\varphi_e(z)\varphi_h(z)|^2 \rangle / a^2. \quad (3)$$

B. Radiative lifetime effects of excitonic center-of-mass motion in the plane of the CQW

Momentum conservation considerations for radiative recombination dictate that in a perfect 2D excitonic system in the limit of zero temperature,¹³ only excitons with zero translational wave vector ($\underline{K}=0$) contribute to the radiative recombination rate. Under such idealized conditions all units cells within the layer contribute to the transition which is thus characterized by a coherent transition strength which is δ -like in energy, with a strength given by

$$F_{\text{ex}}^{2D} = f_0 V \langle |\Phi_{\text{ex}}(\rho=0)|^2 \rangle_{\text{av}}, \quad (4)$$

where f_0 is the interband dipole matrix element per unit cell connecting conduction- and valence-band Bloch states and V is the total volume of the QW layer.

In real QW's at finite temperatures, the perfect coherence of the component of the excitonic wave function describing in plane center-of-mass (C.M.) motion is destroyed (a) by disorder scattering from interface fluctuations and other defects, (b) by acoustic-phonon scattering, and (c) by exciton-exciton scattering at high excitation densities. These processes can be modeled by sharing the δ -like oscillator strength of Eq. (4) over all the allowed 2D translational momentum states which are contained within a homogeneous linewidth $\Gamma_{\text{hom}}(T)$. $\Gamma_{\text{hom}}(T)$ here corresponds to the Heisenberg inverse of the mean lifetime of an exciton in a given translational momentum state and will be dependent both on sample temperature and on sample quality. This approach yields a modified transition strength for $\underline{K} \approx 0$ excitonic transitions given by

$$F_{\text{ex}}^{2D} = \frac{f_0 \langle |\varphi_e(z)\varphi_h(z)|^2 \rangle h^2}{\pi^2 M a^2 \Gamma_{\text{hom}}(T)}, \quad (5)$$

where M is the sum of the electron and hole in-plane masses. Defining a coherence area $A_c = h^2/2\pi M \Gamma_{\text{hom}}(T)$ for the coherence of the in-plane translational component of the wave function gives

$$F_{\text{ex}}^{2D} = 2f_0 \langle |\varphi_e(z)\varphi_h(z)|^2 \rangle A_c / \pi a^2. \quad (6)$$

For excitons localized in regions of the QW with a locally wide well width, but with a lateral area A_l which is less than A_c , the transition strength is given by Eq. (6) but with A_c replaced by A_l .

For an exciton population at a finite temperature T (described by a Maxwellian distribution in energy), only the fraction $R(T) = 1 - \exp[-\Gamma_{\text{hom}}(T)/kT]$ of the population with translational energies less than $\Gamma_{\text{hom}}(T)$ can

recombine whilst satisfying momentum conservation. This finally leads to an expression for the effective oscillator strength governing radiative decay given by

$$F_{x,\text{eff}}^{2D} = 2f_0 |\langle \varphi_e(z) | \varphi_h(z) \rangle|^2 A_c R(T) / \pi a^2 \quad (7)$$

which determines the radiative lifetime according to¹³

$$\tau_r = \frac{2\pi\epsilon_0 m_0 c^3}{n e^2 \omega^2 F_{x,\text{eff}}^{2D}}, \quad (8)$$

where n is the refractive index and ω is the optical frequency of the radiative transition.

In the experiments reported here, all of the quantities with the exception of A_c in this last expression are known or calculable. A measurement of the absolute lifetime thus enables the coherence area of the exciton to be measured, and in the case where $A_c > A_l$, the mean localization island size can be deduced.

In the limit $kT \gg \Gamma_{\text{hom}}(T)$, Eq. (7) predicts a lifetime linearly proportional to temperature, with a field dependence at a given temperature determined solely by the changing overlap integral for relative e - h motion. For $kT \ll \Gamma_{\text{hom}}(T)$, a radiative lifetime proportional to $\Gamma_{\text{hom}}(T)$ is expected, with higher structural quality samples giving larger coherence areas and hence faster recombination times. In this latter limit the recombination time at a given temperature may exhibit an extra

field dependence (over and above that predicted due to the changes in the relative motion overlap integral), due to field dependence of exciton scattering and/or localization effects.

III. EXPERIMENTAL DETAILS

The experiments were performed on a GaAs- $\text{Al}_x\text{Ga}_{1-x}\text{As}$ coupled quantum-well structure (4) grown by molecular-beam epitaxy (MBE) on a Si-doped (100) GaAs substrate with the following parameters (Fig. 1): a 0.5- μm Si-doped buffer layer (10^{18} cm^{-3}); 20 nm $\text{Al}_{0.3}\text{Ga}_{0.7}\text{As}$; 20 nm GaAs; 40 nm $\text{Al}_{0.3}\text{Ga}_{0.7}\text{As}$; 4.8 nm GaAs; 1.6 nm $\text{Al}_{0.3}\text{Ga}_{0.7}\text{As}$; 4.8 nm GaAs; and 40 nm $\text{Al}_{0.3}\text{Ga}_{0.7}\text{As}$. A perpendicular electric field was applied by means of a 100-nm-thick sputtered indium tin oxide (ITO) Schottky barrier contact to the front surface of the sample and an indium alloy contact to the back surface. The ITO layer formed on antireflection coating at 800 nm. The sample parameters above were used for the lifetime modeling and were determined by refining the nominal growth parameters by means of a comparison of the envelope-function calculations with the transition energies measured in cw photoluminescence excitation (PLE) experiments as described in detail in Ref. 4.

The sample was mounted in a continuous-flow cryostat and excited by light from a synchronously mode-locked argon-ion pumped Styryl-8 dye laser at a wavelength of 735 nm (i.e., $\approx 90 \text{ meV}$ above the $n=1$ exciton line). The dye-laser produced 2-ps-duration pulses (measured using a second-harmonic autocorrelator) with a full width at half maximum (FWHM) linewidth of 0.5 meV FWHM. The luminescence was collected at 45° to the sample surface and dispersed using a 0.25-m grating monochromator which was set to pass only the integrated excitonic luminescence from the coupled quantum well. The output of the monochromator was detected and temporally dispersed using a high-sensitivity wide-dynamic photon-counting streak camera system described in detail elsewhere.¹⁴

Pump densities corresponding to peak areal exciton concentrations of $\approx 2 \times 10^9 \text{ excitons/cm}^2$ were used. This is a factor of ≈ 500 lower than the threshold for hot-phonon effects in GaAs MQW's,¹⁵ and at least 2 orders of magnitude below the threshold for excitonic nonlinear effects.

IV. RESULTS

A. Variation of luminescence lifetime as a function of applied field

Time-resolved luminescence profiles taken at 4.2 K (with the sample immersed in liquid helium) for different values of applied bias are shown in Fig. 2. The zero net electric-field bias of +1.05 V (due to the built-in field of the Schottky contact) was determined from the minimum Stark shift in the luminescence line position. A zero-field luminescence lifetime of 151 ps was obtained from a least-squares fit to the exponential decay. As expected, a strong increase in luminescence lifetime was observed as

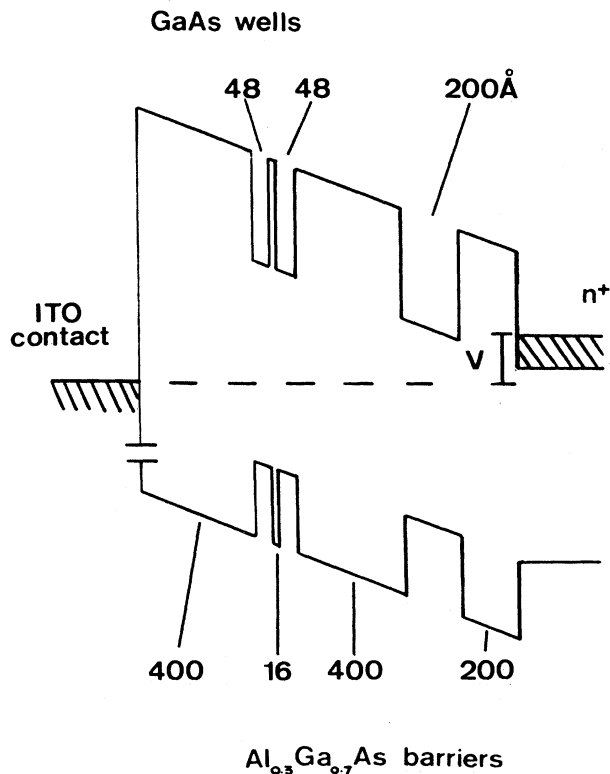


FIG. 1. Schematic of the sample structure. All dimensions in angstroms.

the applied bias was reduced, corresponding to an increase in the actual field across the structure.

Varying the excitation density over more than an order of magnitude resulted in no change in the measured lifetimes and even the fastest luminescence decay curves were exponential over more than 3 orders of magnitude before being lost in the instrumental noise. The nonexponential decay profiles¹⁶ previously observed using similar CQW structures in a p - i - n diode (but pumping with a photon energy above the $\text{Al}_x\text{Ga}_{1-x}\text{As}$ barrier band gap) were not seen here. We obtained identical lifetimes with excitation at 755 nm (which corresponds to a decrease in the initial excess carrier energy by a factor of ≈ 2 to 45 meV).

If exciton-exciton scattering processes were contributing to the observed lifetimes [as previously reported in higher excitation density studies of 12-nm QW's (Ref. 17)], strongly nonexponential decay profiles would be expected due to the reducing exciton density during recombination. Similar profiles would result if the exciton population were not in thermal equilibrium with the lattice as the factor $R(T)$ would change (by a factor of ≈ 2 for a 10-K change in exciton temperature) leading to a decay constant decreasing with time after excitation. We conclude, therefore, that our measured decay profiles are characteristic of a monomolecular radiative excitonic decay process, from an exciton population which is in

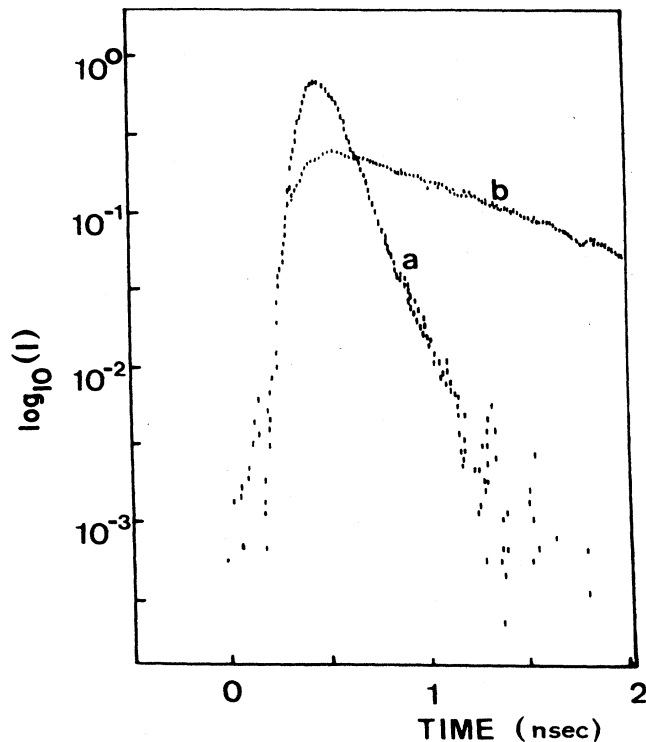


FIG. 2. Typical time-resolved profiles of the heavy-hole luminescence intensity I taken at 4.2 K. (a) Zero perpendicular field. (b) Perpendicular field of 53 kV/cm.

thermal equilibrium with the lattice throughout the period over which the decay constants were measured.

Figure 3(a) shows the calculated variation of the lifetime enhancement factor (LEF), defined as τ/τ_0 , versus the applied electric field, where τ_0 is the lifetime measured at zero electric field. Uncertainties in the field distribution in the sample were eliminated by calculating the fields from the measured ground-state exciton Stark shifts. Using these field values the behavior of the energies of the seven higher-lying confined state transitions measured in PLE [Eq. (4)] were also well modeled.

Excellent agreement is obtained between the measured LEF and the envelope-function calculation (but only if the effects of varying the excitonic radius are included) over an order of magnitude variation in oscillator strength and with Stark shifts of up to 22 meV (corresponding to a field of 55 kV cm^{-1}). The integrated exci-

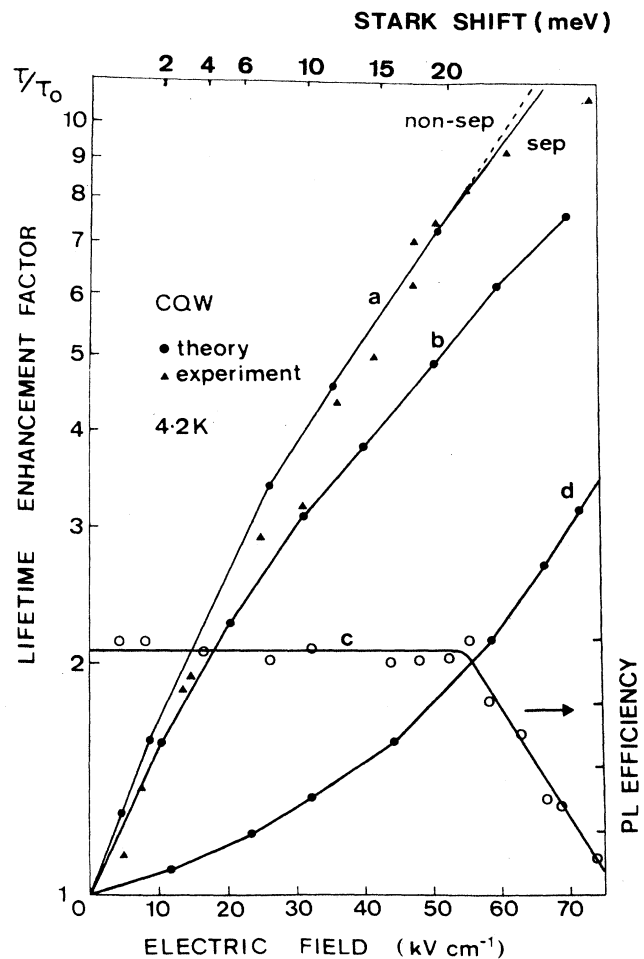


FIG. 3. 4.2-K luminescence data. (a) Results of variational envelope-function calculation including the effects of varying the excitonic in-plane radius. Solid line, separable solution; dashed line, nonseparable solution. (b) Results of the calculation ignoring varying excitonic in-plane radius. (c) PL efficiency. (d) Full variational envelope-function calculation for 10 nm SQW.

tonic luminescence efficiency [Fig. 3(c)] is constant up to this field, confirming that the exciton lifetime is not affected by the field-dependent tunneling processes found elsewhere in MQW structures at high fields.⁸ Furthermore, the close agreement between theory and experiment indicates that the radiative lifetime is identical to the luminescence decay constant and that any field-independent nonradiative processes which may be present in the sample are having a negligible effect on the exciton lifetimes. For fields greater than 55 kV cm^{-1} the lifetime enhancement factor starts to saturate due to the onset of significant nonradiative decay channels as indicated in Fig. 3(c) by the quenching of the excitonic luminescence efficiency, and in this case the luminescence decay time constant underestimates the true radiative decay time constant.

We are unable to distinguish between the accuracies of the separable and nonseparable envelope functions here because their predictions only diverge for high fields where significant nonradiative recombination effects occur. The theoretical LEF curve is not strongly affected by different parallel effective-mass values; using $\mu = 0.049m_0$ gives a difference of only 3% in τ/τ_0 even at $\tau/\tau_0 = 9$. The theoretical curve for a 10-nm SQW [Fig. 3(d)] illustrates the degree of the enhancement of the QCSE in terms of the larger oscillator strength changes which are obtained in the CQW structure. Figure 4 shows the dependence of the calculated expectation value of exciton binding energy and exciton radius a on field.

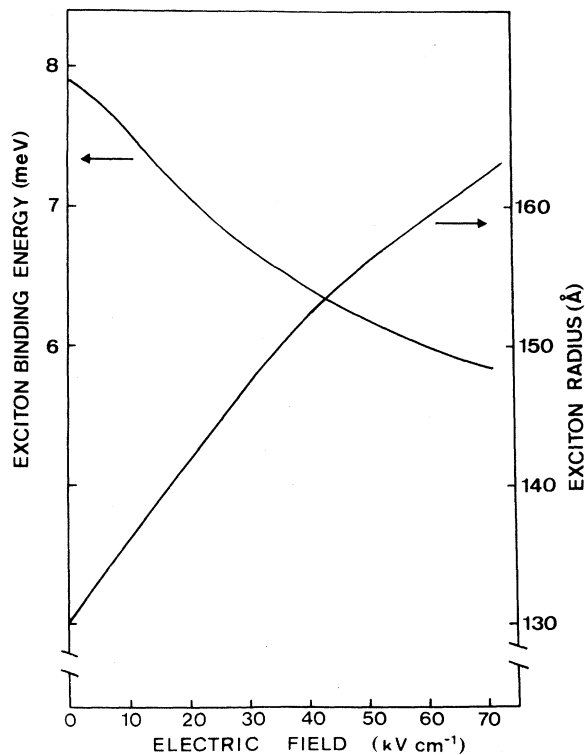


FIG. 4. In-plane excitonic radii and excitonic binding-energy terms as a function of applied field calculated with full variational method and sample parameters from (4).

B. Variation in luminescence lifetime with applied field between 10 and 60 K

Variable temperature measurements show a linear increase in lifetime (Fig. 5) for $30 < T < 60 \text{ K}$, whereas below $T \approx 30 \text{ K}$, a sublinear dependence is observed. Similar behavior was observed by Feldmann *et al.* particularly in a narrower 2.5 nm SQW sample and was tentatively attributed to the effects of exciton localization.

In the CQW samples used in the present work the alloy fluctuations present in the thin barrier layer may act to increase the depth of localization potentials (compared with SQW's), although the results of the variational calculations indicate that the carrier confinement energies are only 0.4 times as sensitive to monolayer fluctuations in the central barrier thickness as they are to monolayer fluctuations in the overall CQW width. The so-called "Stokes shift" of $\approx 2.5 \text{ meV}$ that we measured between the position of the $n=1$ heavy-hole exciton peaks observed in 4.2 K luminescence and in luminescence excitation spectra in this sample is consistent with a transition from localized to delocalized excitonic behavior at $\approx 30 \text{ K}$.

The observed temperature independence of the recombination times for temperatures less than $\approx 30 \text{ K}$ can thus be explained by either of two hypotheses: namely (a) the exciton scattering rates are such that $A_c > A_l$, and the low-temperature exciton lifetimes are determined by a localization limited exciton coherence area and are therefore given by Eq. (5) with A_c replaced by A_l ; or (b) the exciton scattering processes in this sample are of such a strength as to give a rather large homogenous linewidth of the order of 3 meV [so that a transition from the $\Gamma_{\text{hom}}(T) < kT$ regime to the $\Gamma_{\text{hom}}(T) > kT$ regime occurs at $\approx 30 \text{ K}$], and that the resulting exciton coherence area determines the low-temperature lifetime values through

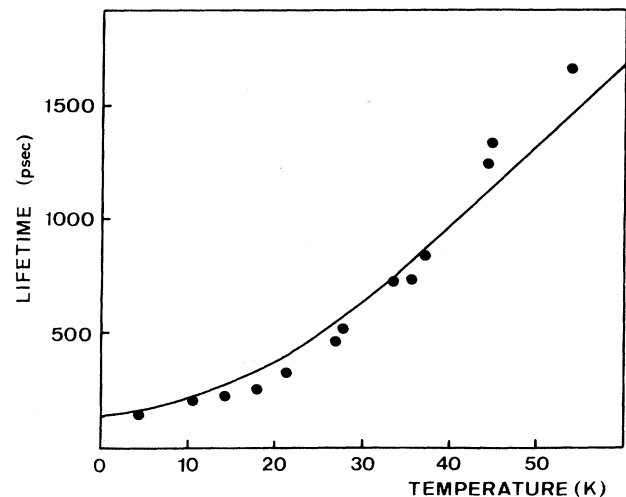


FIG. 5. Dots, measured lifetime vs temperature for the CQW with zero applied field. Solid line, numerical model evaluated for a localization island diameter of 61.5 nm.

Eq. (6), both for localized and delocalized excitons because $A_c < A_l$.

With regard to hypothesis (b), variable temperature time-resolved degenerate four-wave-mixing measurements in 13.5-nm QW structures¹⁸ have yielded homogeneous linewidths of the form $\Gamma_{\text{hom}}(T) = 0.5 + 0.005T$ meV for the heavy-hole exciton line. The increased scattering from alloy disorder in the thin barrier layer might be expected to result in a larger temperature-independent component to $\Gamma_{\text{hom}}(T)$ in a CQW but, conversely, the sample used in Ref. 18 showed pronounced extrinsic structure in PL (effects not seen in our sample), suggesting the presence of a substantial impurity concentration, and a comparison of the relative contributions of disorder scattering in the two structures is not straightforward.

The absence of significant nonradiative channels in the CQW, however, allows us to make a meaningful comparison between the *absolute* values of the recombination lifetimes and the predictions of Eq. (6). Using a value of

$f_0 = 0.802$ (Refs. 19 and 20) the measured low-temperature limit of the exciton lifetime corresponds to an excitonic coherence area of $5.55 \times 10^{-15} \text{ m}^2$. If hypothesis (b) applies, this in turn corresponds to a low-temperature limit of $\Gamma_{\text{hom}}(T)$ of only 0.071 meV [compared with the ≈ 0.5 meV value reported for a 13.5-nm QW (Ref. 18)]. Assuming the $5 \mu\text{eV/K}$ sample-independent temperature varying component of $\Gamma_{\text{hom}}(T)$ of Ref. 17, this would lead to the transition between the $\Gamma_{\text{hom}}(T) < kT$ and the $\Gamma_{\text{hom}}(T) > kT$ regimes occurring at ≈ 1 K as opposed to the value of ≈ 30 K observed here and we therefore conclude that hypothesis (a) applies and the low-temperature lifetimes are dominated by exciton localization effects in this sample.

The solid curve in Fig. 5 is a numerical fit to the zero-field data calculated using a 4.2-K Boltzmann distribution of excitonic energies and an excitonic translational momentum density-of-states function which corresponds to the localization islands occupying 50% of the total CQW area. The following values were used: $f_0 = 0.802$, an in-plane exciton reduced mass $\mu = 0.046m_0$, exciton localization energy $E_{\text{loc}} = 2.5$ meV, $\Gamma_{\text{hom}}(T) = 0.50 + 0.005T$,¹⁷ and a mean exciton localization island diameter of 84 nm.

For the typical localization energies found in QW samples, we find the predicted lifetime temperature dependence to be largely insensitive to the values of $\Gamma_{\text{hom}}(T)$ assumed, because the lifetimes are dominated by localization effects up to temperatures that are large compared to $\Gamma_{\text{hom}}(T)/k$. Whilst for $T > \approx 40$ the fitting procedure essentially involves no free parameters, at 4.2 K the lifetime is determined wholly by the mean localization island size assumed and it can thus be seen that careful TRPL measurements can be used to provide a rather direct measure of the lateral scale of interface roughness for comparison with theoretical models of epitaxial growth dynamics.

Such a measurement is sensitive to interface fluctuations in the range ≈ 26 nm (the zero-field exciton diameter) to ≈ 170 nm [the diameter of the exciton coherence area corresponding to the case where the low-temperature limit of the homogenous linewidth is given purely by the Heisenberg inverse of the exciton radiative lifetime calculated by substituting Eq. (6) in Eq. (8)].

At higher temperatures the field dependence of the exciton lifetime was found to be well described by the relative motion part of the exciton wave function alone (Fig. 6), and no field-dependent localization effects were seen. The ≈ 1.5 -nsec upper limit of measurable lifetimes (set by the laser repetition rate) prevented a more detailed study of this effect from being made.

V. CONCLUSIONS

For the first time the predicted enhancement of the changes in oscillator strength and luminescence lifetime in CQW's has been observed and accurately modeled. The quantitative nature of this study demonstrates that the variation of the excitonic wave-function diameter

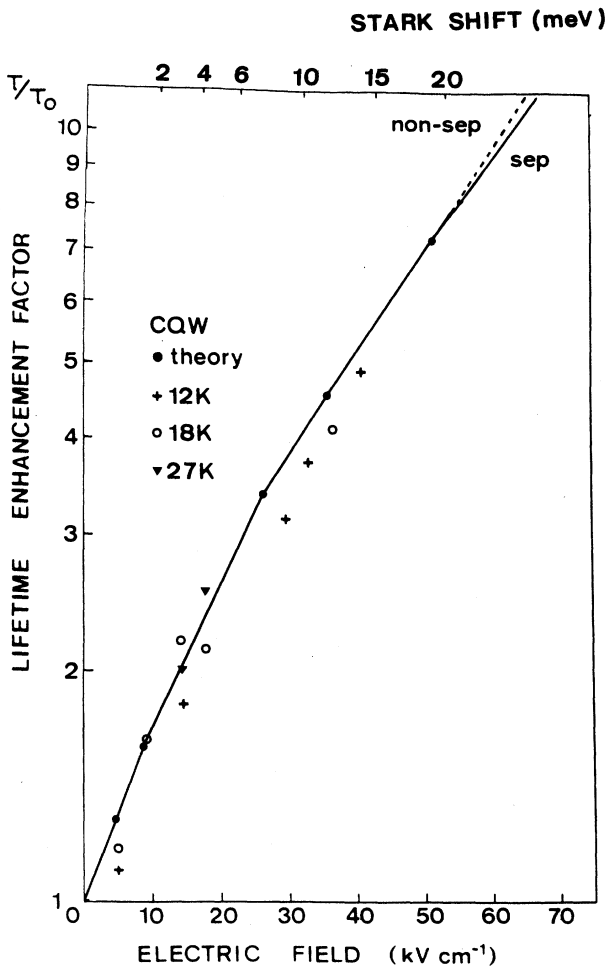


FIG. 6. Lifetime enhancement factor τ/τ_0 at different temperatures. Solid line, full variational envelope-function calculation for CQW.

with perpendicular field is now well understood and that the envelope-function approach is therefore appropriate for the calculation of both Stark shifts and oscillator strengths for the design and optimization of electro-absorption device structures.

The temperature dependence of exciton lifetimes is shown to be well described by the coherence area effects previously reported in SQW structures, and the positive identification of localization limited lifetimes has enabled

the mean island diameter for excitonic localization in these structures to be measured as 84 nm.

ACKNOWLEDGMENTS

This work was supported by the United Kingdom Opto-Electronic Research Scheme and by the Science and Engineering Research Council. We would also like to thank Dr. T. M. Kerr (GEC Research Limited, Hirst Research Centre) for the provision of samples.

-
- ¹R. Dingle, *Festkorperprobleme XV*, 21 (1975).
²D. A. B. Miller, D. S. Chemla, T. C. Damen, A. C. Gossard, W. Wiegmann, T. H. Wood, and C. A. Burrus, *Phys. Rev. Lett.* **53**, 2173 (1984).
³Y. J. Chen, E. S. Koteles, B. S. Elman, and C. A. Armiento, *Phys. Rev. B* **36**, 4562 (1987).
⁴S. R. Andrews, C. M. Murray, R. A. Davies, and T. M. Kerr, *Phys. Rev. B* **37**, 8198 (1988).
⁵J. A. Kash, E. E. Mendez, and H. Morkoç, *Appl. Phys. Lett.* **46**, 173 (1985).
⁶J. A. Kash, E. E. Mendez, and H. Morkoç, *Appl. Phys. Lett.* **46**, 173 (1985).
⁷H. J. Polland, L. Schultheis, J. Kuhl, E. O. Gobel, and C. W. Tu, *Phys. Rev. Lett.* **55**, 2610 (1985).
⁸K. Kohler, H. J. Polland, L. Schultheis, and C. W. Tu, *Phys. Rev. B* **38**, 5496 (1988).
⁹R. C. Miller and D. A. Kleinmann, *J. Lumin.* **30**, 520 (1985).
¹⁰A. S. Plaut, J. Singleton, R. J. Nicholas, R. T. Harley, S. R. Andrews, and C. T. B. Foxon, *Phys. Rev. B* **38**, 1323 (1988).
¹¹D. A. Broido and L. J. Sham, *Phys. Rev. B* **34**, 3917 (1986).
¹²C. Priester, G. Allen, and M. Lunnoo, *Phys. Rev. B* **30**, 7302 (1984).
¹³J. Feldmann, G. Peter, E. O. Gobel, P. Dawson, K. Moore, C. T. B. Foxon, and R. J. Elliott, *Phys. Rev. Lett.* **59**, 2337 (1987); **60**, 243(E) (1988).
¹⁴R. Eccleston and C. C. Phillips, *J. Phys. E* **22**, 409 (1989).
¹⁵J. Shah, *IEEE J. Quantum Electron.* **QE-22**, 1728 (1986).
¹⁶S. Charbonneau, M. L. W. Thewalt, E. S. Koteles, and B. Eltman, *Phys. Rev. B* **38**, 6287 (1988).
¹⁷J. Kuhl, A. Honold, L. Schultheis, and C. W. Tu, *Topical Meeting on Quantum Wells for Optics and Optoelectronics*, Vol. 10 of *1989 Technical Digest Series* (Optical Society of America, Washington, D.C., 1989), pp. 46–49.
¹⁸L. Schultheis, A. Honold, J. Kuhl, K. Kohler, and C. W. Tu, *Phys. Rev. B* **34**, 9027 (1986).
¹⁹M. Shinada and S. Sugano, *J. Phys. Soc. Jpn.* **21**, 1936 (1966). f_0 values were calculated by substituting the measured absorption data of Ref. 20 into the expressions contained in this work.
²⁰D. S. Chemla, D. A. B. Miller, P. W. Smith, A. C. Gossard, and W. Wiegmann, *IEEE J. Quantum. Electron.* **QE-20**, 265 (1984).